

Article

Fatigue Strength Assessment of Single-Sided Girth Welds in Offshore Pipelines Subjected to Start-Up and Shut-Down Cycles

Yan Dong ^{1,2,3} , Guanglei Ji ¹, Lin Fang ⁴ and Xin Liu ^{1,*} 

¹ Yantai Research Institute of Harbin Engineering University, Harbin Engineering University, Yantai 264000, China

² College of Shipbuilding Engineering, Harbin Engineering University, Harbin 150000, China

³ HEU-UL International Joint Laboratory of Naval Architecture and Offshore Technology, Harbin Engineering University, Harbin 150000, China

⁴ COOEC Subsea Technology Co., Ltd., Shenzhen 518000, China

* Correspondence: xin.liu@hrbeu.edu.cn

Abstract: During the service life of offshore pipelines, many start-up and shut-down cycles take place, possibly leading to significant cyclic loads. Fatigue failure may occur, resulting in serious environmental pollution and loss of property. The study aims to assess the fatigue strength of single-sided girth welds in offshore pipelines under these specific fatigue loads. The longitudinal stress range caused by the variation of the pipeline's internal pressure and temperature is calculated. The effective notch strain approach is used to assess the fatigue strength of welds. The plastic behaviour of the weld root is investigated for a study case to justify the use of low-cycle fatigue assessment approaches. The effect of weld root geometry on the notch stress factor is studied to identify the dominant geometrical parameters. The fatigue strength of the study case is assessed, and some limitations of the assessment are discussed. The results show that the plastic behaviour of the weld root is only significant for severe local stress concentrations, which is mainly governed by the axial misalignment, weld root angle and the weld root bead width. If the fatigue damage at failure is 0.1, a limited number of start-up and shut-down cycles are allowed during the service life of the pipeline for the study case, indicating the necessity of fatigue strength assessment.

Keywords: fatigue strength; offshore pipelines; girth welds; low cycle fatigue



Citation: Dong, Y.; Ji, G.; Fang, L.; Liu, X. Fatigue Strength Assessment of Single-Sided Girth Welds in Offshore Pipelines Subjected to Start-Up and Shut-Down Cycles. *J. Mar. Sci. Eng.* **2022**, *10*, 1879. <https://doi.org/10.3390/jmse10121879>

Academic Editor: Bruno Brunone

Received: 25 October 2022

Accepted: 20 November 2022

Published: 3 December 2022

Publisher's Note: MDPI stays neutral with regard to jurisdictional claims in published maps and institutional affiliations.



Copyright: © 2022 by the authors. Licensee MDPI, Basel, Switzerland. This article is an open access article distributed under the terms and conditions of the Creative Commons Attribution (CC BY) license (<https://creativecommons.org/licenses/by/4.0/>).

1. Introduction

Subsea pipelines are subjected to fatigue loading in operation conditions, which include those induced by motions of floating platforms, free span vortex-induced vibrations, and thermal cycles. These fatigue loadings may result in significant fluctuating stresses acting on the girth welds of pipelines, leading to fatigue failure. The fatigue strength of subsea pipelines has been a major concern.

An increasing number of high-pressure and high-temperature (HPHT) offshore pipelines have been applied in recent years because more and more HPHT oil and gas fields are being developed. HPHT applications of 150 °C and 68.95 MPa are common nowadays, and more severe HPHT operating conditions also exist [1]. Subsea pipelines under HPHT operating conditions have to face various challenges. The global lateral buckling may happen because of the high compressive axial force when the pipelines are laid on the seabed and heated, but the axial extensions are restrained by the soil [2]. The pipelines are subjected to a number of cycles of start-up and shut-down through the design life of an offshore field. The pipeline walking, i.e., global axial movement can be triggered by the start-up and shut-down cycles in some cases, leading to some problems that may endanger the pipeline system [3]. The HPHT conditions can increase the corrosion rate of

the pipeline significantly [4]. Relative large stress ranges may take place due to the start-up and shut-down process, resulting in low cycle fatigue (LCF) of the pipeline [5].

In the present study, the focus is given to the fatigue damage of single-sided girth welds in offshore pipelines caused by the start-up and shut-down cycles. Since the loading cycles may be significant, the LCF approaches instead of high cycle fatigue (HCF) approaches are recommended. Compared with the HCF approaches, the LCF approach needs more computational efforts. The LCF approaches are generally classified into two types, one based on S-N curves and linear damage rule, and another relies on fatigue crack propagation analyses. The strain parameters or the elastic-plastic fracture mechanics are used in these approaches. The first type of approach includes the pseudo hotspot stress approach [6,7], structural strain approach [8,9], notch strain approach [10,11] and effective notch strain approach [12,13]. The approaches belonging to the second type usually use the cyclic J-integral [14–17] and the cyclic crack tip opening displacement [18,19] as the driving forces of crack growth. The first type of approach is easier to use in practice because a lower number of parameters is usually involved, and the calculation is more efficient, while the second type of approach is closer to the physical fatigue process.

Although many approaches have been developed for the LCF problem, the study on fatigue strength assessment of offshore pipelines subjected to start-up and shut-down cycles is rare. One reason may be that the special fatigue problem can be coupled with global buckling, which complicates the problem. When the pipeline is heated, global buckling may happen and can lead to a release of the global compressive force. Furthermore, the associated bending of the pipeline can either increase or decrease the local stress depending on the location of interest. In the present study, it is assumed that the pipeline remains straight during start-up and shut-down cycles, and the effects of global buckling are ignored.

The study on the fatigue strength assessment under these specific cyclic loads may contribute to improving the safety of subsea pipelines. The allowed number of cycles can be obtained from the analyses, which is valuable for the management of offshore oil and gas fields.

In the present study, the fatigue strength assessment of single-sided girth welds in offshore pipelines subjected to start-up and shut-down cycles is performed. The calculation of the longitudinal stress range due to the start-up and shut-down cycle and the effective notch strain approach is introduced. For a specific study case, the plastic behaviour of the weld root is investigated to justify the use of the LCF approach, and the effect of weld root geometry on the notch stress factor is studied to identify the dominant geometrical parameters. The fatigue strength of the study case is assessed, and some limitations of the assessment are discussed.

2. Methods

The methods involved in the fatigue strength assessment are introduced in this section. The fatigue loads acting on the welds are determined analytically. The effective notch strain approach is used for the fatigue strength assessment. The finite element method (FEM) and the analytical method are combined to calculate the effective notch strain.

2.1. Start-Up and Shut-Down Load Cycles

The stress components in pipelines are longitudinal (axial) stress, hoop (circumferential) stress and radial stress. Since fatigue cracks are usually initiated at girth welds and propagate along the direction of the weld line and the thickness, the stress component normal to the potential crack plane, i.e., the longitudinal stress, is of interest.

In the present study, the pipeline is assumed to be fully constrained. In other words, there is no longitudinal movement when the internal pressure or temperature is increased. The assumption can result in more conservative longitudinal stresses.

The longitudinal stress for the installation condition $\sigma_{l,ins}$ can be calculated by [1]:

$$\sigma_{l,ins} = \frac{F_{res} + P_{i,ins}A_i - P_eA_e}{A_s} \tag{1}$$

where F_{res} is the installation residual lay tension, $P_{i,ins}$ is the internal pressure of the pipe during installation, A_i is the internal bore area of the pipe, P_e is the external pressure of the pipe, A_e is the external area of the pipe, A_s is the cross-sectional area of the pipe.

When the temperature and pressure are increased to the operational condition, the pipeline tends to expand longitudinally. However, the pipeline is fully restrained, and thus, the compressive longitudinal stress is developed. For a fully restrained pipeline, the longitudinal stress is caused by the Poisson’s ratio effect of hoop and radial stresses and the thermal effect [1]:

$$\sigma_l = \frac{2\nu(P_iA_i - P_eA_e)}{A_s} - E\alpha(T_{op} - T_a) \tag{2}$$

where σ_l is the longitudinal stress, E is Young’s modulus, ν is the Poisson’s ratio, P_i is the operational internal pressure, α is the thermal expansion coefficient of pipe material, T_{op} is the operational temperature and T_a is the ambient temperature at installation.

Taking the longitudinal stress for the installation condition as the initial condition, the longitudinal stress for the operational condition can be calculated by:

$$\sigma_{l,op} = \sigma_{l,ins} + \frac{2\nu(P_i - P_{i,ins})A_i}{A_s} - E\alpha(T_{op} - T_a) \tag{3}$$

The longitudinal stress range caused by the start-up and shut-down load cycle is

$$\Delta\sigma_l = \left| \sigma_{l,op} - \sigma_{l,ins} \right| = \left| \frac{2\nu(P_i - P_{i,ins})A_i}{A_s} - E\alpha(T_{op} - T_a) \right| \tag{4}$$

For the fully restrained condition, increasing the operating internal pressure and increasing the operating temperature has the opposite effect on the longitudinal stress range. Increasing the operating internal pressure means increasing the hoop stress, leading to tensile longitudinal stresses due to Poisson’s ratio effect for the fully restrained condition. However, increasing the operating temperature results in compressive longitudinal stress because the extension is restrained.

The assumption of a fully restrained condition is conservative, and the fatigue strength assessment based on this assumption is representative. If the pipeline is free at the end, the variation of longitudinal stress is limited around the end and continuously increases toward the centre of the pipeline until the fully restrained condition is developed. In the present study, only the fully restrained condition is considered.

Note that significant compressive stress can be developed in the operational condition, implying the stress variation due to the start-up and shut-down load cycle is mainly in the regime of the compressive stress. It does not mean the fatigue problem is less important because the local welding-induced residual stresses around the welds may approach the yield stress of the material, which can significantly improve the local mean stress.

2.2. Fatigue Strength Assessment

The effective notch strain approach is extended from the effective notch stress approach from the HCF regime. It can be used to deal with LCF and HCF problems and is employed in the present study. Compared with the notch train approach, the effective notch strain approach is easier to be applied in practice [13]. Detailed information on local geometry and residual stresses is not required, and it can result in the total fatigue life instead of the crack initiation life.

The method for the estimation of the effective notch strain, which is proposed by Dong et al. [13], is used. The method is simpler than the elastic–plastic finite element method. It can be divided into two steps. The first step is to calculate the effective notch

stress as recommended by the International Institute of Welding [20]. The weld toe and root are rounded by a fictitious notch whose radius is $\rho_f = 1$ mm for welded steel structures with a thickness larger than 5 mm, as shown in Figure 1. The FEM is usually used. The maximum first principal stress along the notch is taken as the effective notch stress.

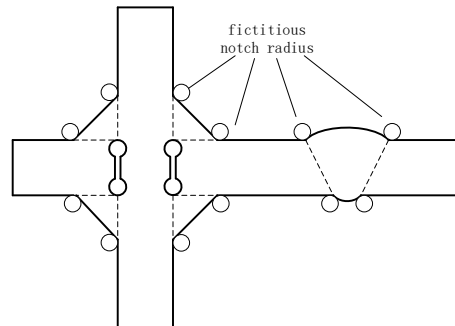


Figure 1. Fictitious notch rounding [20].

The second step is to convert the elastic stress to the elastic–plastic strain. The step is mainly based on the plane strain equivalent strain energy density approach [21,22]. The plane strain state is assumed, implying that the strain component along the notch is zero and a biaxial stress state exists at the notch tip when the notched component is remotely loaded. The uniaxial cyclic stress–strain curve of the material is assumed to follow the Ramberg–Osgood relation:

$$\varepsilon = \frac{\sigma}{E} + \left(\frac{\sigma}{K'}\right)^{\frac{1}{n'}} \tag{5}$$

where K' is the cyclic strength coefficient, n' is the cyclic strain hardening exponent and E is the elastic modulus. According to [23], the above curve should be transformed into the plane strain curve by using:

$$\begin{cases} \sigma_1 = \frac{\sigma}{\sqrt{1-\mu+\mu^2}} \\ \varepsilon_1 = \frac{\varepsilon(1-\mu^2)}{\sqrt{1-\mu+\mu^2}} \\ \mu = \frac{1}{2} - \left(\frac{1}{2} - \nu\right) \frac{\sigma}{E\varepsilon} \end{cases} \tag{6}$$

where stress and strain with a subscript 1 represent the first principal quantities, ν is the Poisson’s ratio and μ is the generalised Poisson’s ratio. The data points in the uniaxial cyclic stress–strain curve can be transformed into the data points of $(\sigma_1, \varepsilon_1)$. The plane strain curve can be fitted based on these data points, and the plane strain curve is in the form of:

$$\varepsilon_1 = \frac{\sigma_1}{E} (1 - \nu^2) + \left(\frac{\sigma_1}{K'_1}\right)^{\frac{1}{n'_1}} \tag{7}$$

where K'_1 and n'_1 are the new material properties. The plane strain equivalent strain energy density approach can be expressed by:

$$\frac{\sigma_{eff}^2(1 - \nu^2)}{2E} = \int_0^{\varepsilon_1} \sigma_1 d\varepsilon_1 \tag{8}$$

where σ_{eff} is the effective notch stress. The first principal notch strain ε_1 can be solved by combining Equations (3) and (4). The generalised Poisson’s ratio μ can also be obtained. According to Equation (6), the effective notch strain can be estimated by:

$$\varepsilon_{eff} = \frac{\varepsilon_1 \sqrt{1 - \mu + \mu^2}}{(1 - \mu^2)} \tag{9}$$

Generally, the effective notch strain range is of interest in fatigue strength assessment. The effective notch strain amplitude ϵ_{eff} is obtained by solving Equations (3)–(5), in which the σ_{eff} is the effective notch stress amplitude. The effective notch strain range is twice the effective notch strain amplitude.

The curves of effective notch strain range $\Delta\epsilon_{eff}$ vs. fatigue life N_f for a survival probability of 97.7% can be expressed by:

$$\begin{cases} N_f(\Delta\epsilon_{eff})^{m_1} = C_1 & N_f < 10^4 \\ N_f(\Delta\epsilon_{eff})^{m_2} = C_2 & N_f \geq 10^4 \end{cases} \quad (10)$$

The segment of $N_f < 10^4$ is derived from the LCF test data [12], and the segment of $N_f \geq 10^4$ is derived from the S-N curve of FAT225 for the effective notch stress approach [20]. The relationship between the effective notch strain range and effective notch stress range in the elastic domain is:

$$\Delta\epsilon_{eff} = \frac{\Delta\sigma_{eff}\sqrt{1-\nu+\nu^2}}{E} \quad (11)$$

The values of S-N curve parameters are listed in Table 1, and the S-N curves are shown in Figure 2.

Table 1. S-N curve parameters [13].

S-N Curve Parameter	Value
C_1	1.25×10^{-3}
m_1	3.195
C_2	1.83×10^{-3}
m_2	3

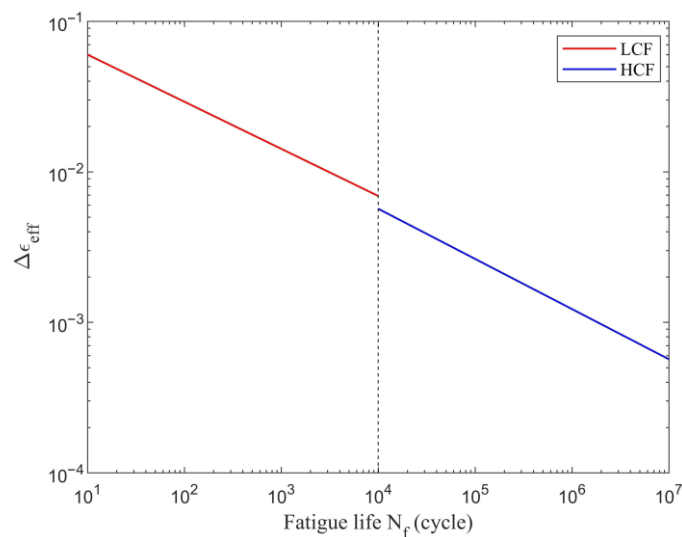


Figure 2. S-N curves for the effective notch strain approach [13].

3. Case Study

The fatigue strength of a specific case is investigated in the present study. The data of the example pipeline are presented in Table 2.

Table 2. Information for the example pipeline.

Modelling Parameters	Unit	Value
Pipeline outer diameter, D_e	mm	355.6
Pipeline wall thickness, t	mm	19.8
Area of steel pipeline’s cross-section, A_s	m^2	0.0209
Internal pressure of installation/shut-down, $P_{i,ins}$	MPa	2
Operating internal pressure, P_i	MPa	20
Operating temperature, T_{op}	$^{\circ}C$	120
Seabed ambient temperature, T_a	$^{\circ}C$	12
Coefficient of thermal expansion, α	$^{\circ}C^{-1}$	1.3×10^{-5}
Young’s modulus, E	MPa	2.06×10^5
Poisson’s ratio, ν	-	0.3
Cyclic strength coefficient, K'	MPa	923
Cyclic strain hardening exponent, n'	-	0.118

According to Equation (4), the longitudinal stress range due to start-up and shut-down cycles is approximately 248.7 MPa. This stress range is considered the nominal stress range $\Delta\sigma_n$ and used in the following fatigue strength assessment.

In the present study, the cyclic mechanical properties of API 5L X65 pipeline steel are used. Detailed information on the material and its mechanical properties can be found in [24]. In fact, the mechanical properties of heat affected zone are more relevant because fatigue cracks are usually initiated from this location. However, the cyclic mechanical properties of heat affected zone are not available. The use of mechanical properties of parent material usually results in the conservative estimation of local strains [25]. Therefore, the mechanical properties of the parent material are still used in the present study.

For offshore pipelines, single-sided girth welds are more relevant in the industry. According to fatigue tests, the fatigue cracks most likely originate from the inside, i.e., the weld root, due to a possible poor weld root profile [26–28]. It has been shown that weld geometry plays a significant role in fatigue strength. It is assumed that the weld has a flush ground weld toe, and only the idealised geometry of the weld root is considered. The weld root geometry is characterised by four parameters, as shown in Figure 3. They are the weld root bead width W_i , weld root bead height h , weld root angle θ and axial misalignment δ . The weld toe bead width W_e is $W_i + 1.15t$, where t is the wall thickness.

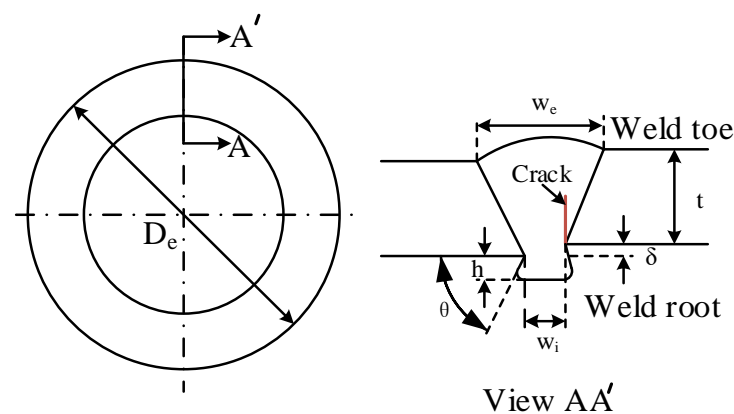


Figure 3. Weld root geometry.

To investigate the effect of weld geometry on the fatigue strength of single-sided girth welds, the weld geometry parameters are varied, as outlined in Table 3.

Table 3. Weld geometry of the single-sided girth weld.

Geometrical Parameters	Unit	Value
Weld root bead width, W_1	mm	4, 6, 8, 10, 12, 14, 16
Weld root bead height, h	mm	2, 3, 4, 5
Weld root angle, θ	°	50, 65, 97.5, 130, 145
Axial misalignment, δ	mm	0, 1, 2, 3

The finite element analyses for the estimation of the effective notch stress are performed using ANSYS [29]. Linear elastic analyses are carried out. The plane strain cross-sectional models, which are usually employed in plate-welded structures [13], are used. A circular notch with a radius of 1 mm is placed at the weld root. The element type of PLANE183 is chosen, and the maximum element size at the circular arc is less than 0.02 mm, which satisfies the requirement of [20]. In the recommendation, the maximum mesh size at the circular arc should be less than 0.25 mm to obtain convergent results. The mesh and boundary conditions of the finite element models are shown in Figure 4. The mesh conditions for $\theta < 90^\circ$ or $\theta \geq 90^\circ$ are both shown in the figure. All the nodes on the right side of the model are fixed, and the nominal stress is applied on the left side of the model. The first principal stress around the notch area is effective notch stress. The total number of nodes and elements varies with the geometrical parameters. The total number of elements is about 17,000, and the total number of nodes is about 50,000.

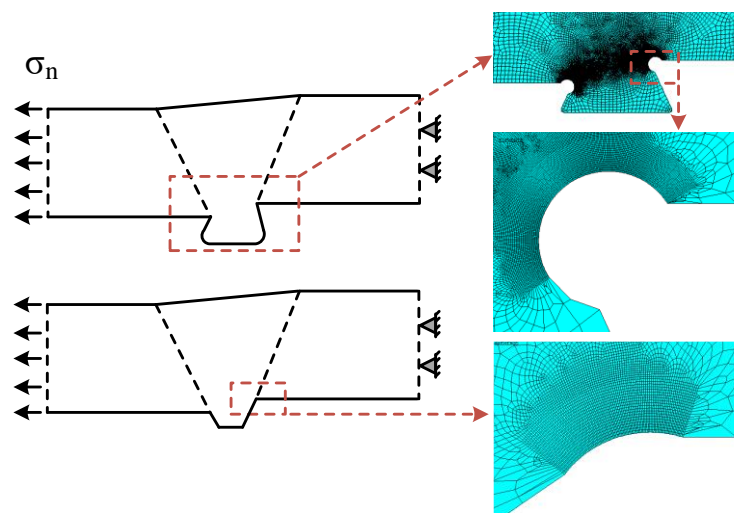


Figure 4. Finite element model for the estimation of the effective notch stress.

4. Results

In this section, the plastic behaviour of the weld root is investigated to justify the use of the LCF approach, and the effect of weld root geometry on the notch stress factor is studied to identify the dominant geometrical parameters. The fatigue strength of the welds is assessed, and the limitations of the assessment are discussed.

4.1. Plastic Behaviour

The effective notch strain approach is extended from the effective notch stress approach to consider the elastic–plastic behaviour. It is suitable for both LCF and HCF. However, the procedure for effective notch strain estimation is still complex, even though a simplified analytical method is used. For the study case, one may be interested in whether it is necessary to use only the effective notch stress approach instead of the effective notch strain approach.

Various notch stress factors K_f is assumed, which is defined by the effective notch stress divided by the nominal stress. For each K_f , the elastic–plastic effective notch strain range

$\Delta\epsilon_{eff}$ and the effective notch strain calculated using Equation (11) $\Delta\epsilon_{eff,e}$ are determined, respectively. The latter quantity is determined under the assumption of the elastic material. The ratio between the two quantities is used to represent the effect of plasticity:

$$r_p = \frac{\Delta\epsilon_{eff}}{\Delta\epsilon_{eff,e}} \tag{12}$$

The results of r_p are shown in Figure 5. The r_p increases nonlinearly with K_f . For the study case, if K_f is less than 4, the r_p is close to 1, indicating that the elastic behaviour dominates. With a further increase in K_f , plastic behaviour becomes more and more important. The result indicates that if the local stress concentration is kept at a low level, the HCF approach can also be used, and the use of the LCF approach is not necessary.

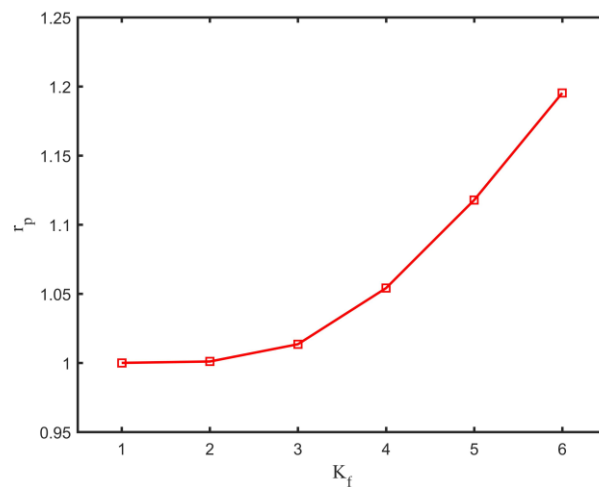


Figure 5. Effect of plasticity for $\Delta\sigma_n = 248.7$ MPa, $K' = 923$ MPa, $n' = 0.118$.

4.2. Effect of Weld Geometry

The weld geometry has a significant impact on K_f . Some results of K_f for different weld geometries are illustrated in this section. The K_f is calculated using FEM. An example of the first principal stress contour is shown in Figure 6.

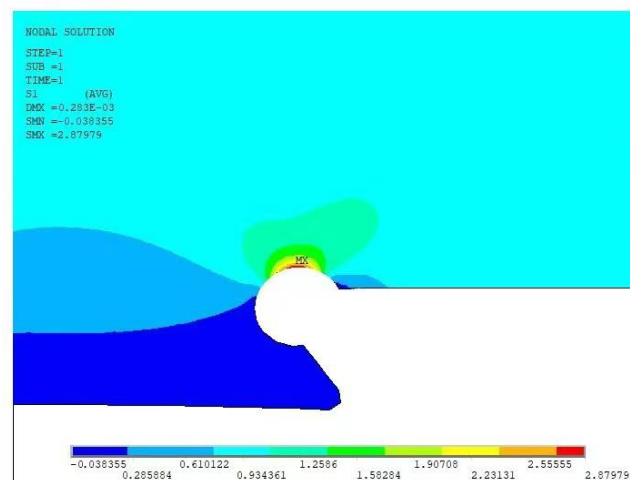


Figure 6. An example of the first principal stress contour (nominal stress is 1 MPa).

The effect h and W_i on K_f is shown in Figures 7 and 8. The effect of h is not as significant as the effect of W_i . The K_f is almost unchanged with the increase of h . The K_f increases rapidly with W_i when W_i is small but tends to approach a plateau value with a large W_i .

The h has a minor effect on the plateau value. The lower h results in a slightly lower plateau value. The effect of W_i may be explained by the development of the eccentricity around the weld. Because of the unsymmetrical weld profile between the weld root and toe, the eccentricity of the neutral line exists around the weld [30]. With the increase of W_i , the eccentricity effect, i.e., local bending, is gradually developed. The fully developed eccentricity effect is similar to the problem of axial misalignment [31].

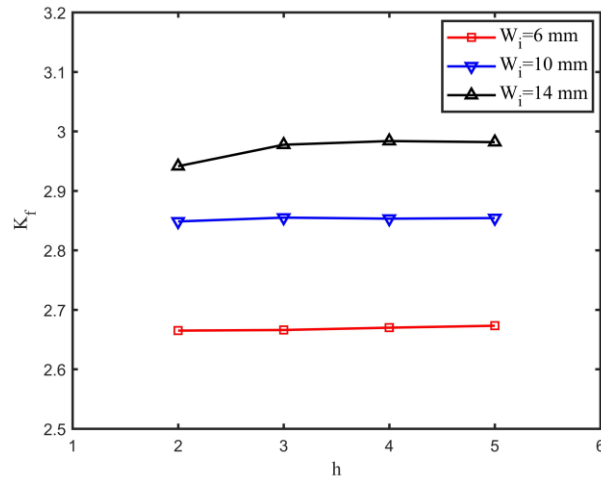


Figure 7. The effect of weld root bead height h ($\delta = 0, \theta = 50^\circ$).

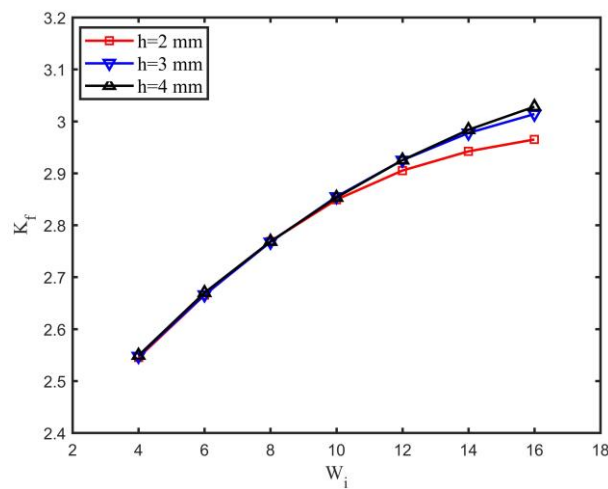


Figure 8. The effect of weld root bead width W_i ($\delta = 0, \theta = 50^\circ$).

The effects of weld root angle and axial misalignment are more significant, as shown in Figures 9 and 10. The K_f decreases linearly with θ and increases linearly with δ . The effect of δ is the most significant among the four geometrical parameters. The K_f can be higher than four if δ is higher than 2 mm. The dangerous conditions are those with a low θ and a high δ .

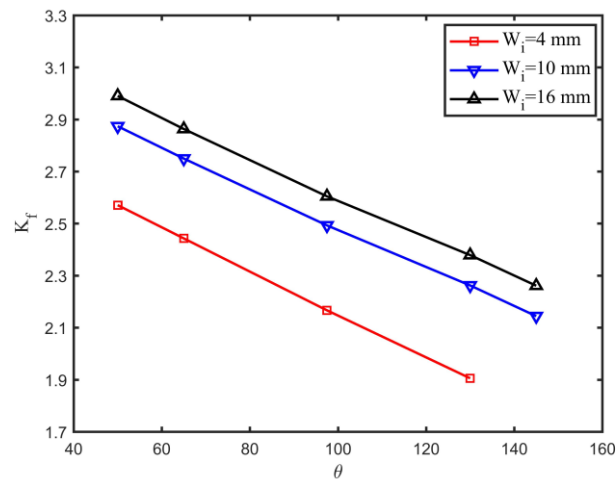


Figure 9. The effect of weld root angle ($\delta = 0$, $h = 2$ mm).

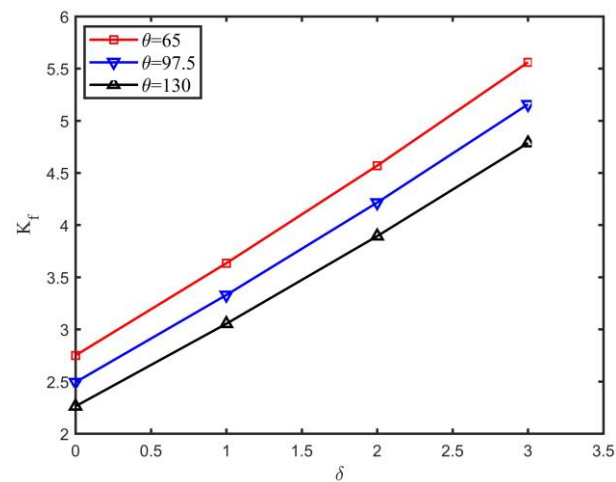


Figure 10. The effect of axial misalignment ($h = 2$ mm $W_i = 10$ mm).

4.3. Fatigue Strength

There are still some problems to be addressed to assess the fatigue strength of single-sided girth welds in offshore pipelines subjected to start-up and shut-down cycles. Firstly, the representative number of cycles should be assumed. The number of these stress cycles is usually up to several hundred during the design life of the offshore field [5]. However, knowledge of the exact number is not available. The number may be subjected to significant uncertainty. Statistical analyses should be performed based on the relevant data collected from various offshore fields. A representative number of cycles, which corresponds to a low level of probability of exceedance, may be employed.

Secondly, representative values of weld geometrical parameters should be assumed. The weld geometry is subjected to significant uncertainty. The representative values of some geometrical parameters can be assumed based on the worst-case scenario or the acceptance tolerance of fabrication. The notch radius of 1 mm is based on the worst-case scenario [20]. The fabrication tolerance for δ is less than 0.1t or a maximum 3 mm ($t =$ wall thickness) [32]. However, the values of other parameters are not available. For other parameters that have a significant effect on the stress concentration, a statistical analysis of the data obtained from the measurement of the weld geometry is needed.

Thirdly, the effect of corrosion and the environment should be considered. The wall thickness, weld geometry and material properties can be changed during the service life due to corrosion. Using the values associated with the initial stage of the service life seems inappropriate. Additionally, the stress cycles are associated with significant thermal cycles,

which may invalidate the traditional approaches for fatigue strength assessment because these approaches are usually developed under room temperatures with minor variation.

For the study case, the following assumptions on the values of geometrical parameters are made: $W_i = 10$ mm, $h = 2$ mm, $\theta = 90^\circ$ and $\delta = 2$ mm. The value of δ is equal to the tolerance for fabrication. The effective notch strain approach introduced in Section 2.2 is still used despite possible invalidation of the approach. The corrosion effects are ignored. The fatigue damages for different numbers of start-up and shut-down cycles N_{ss} are shown in Figure 11.

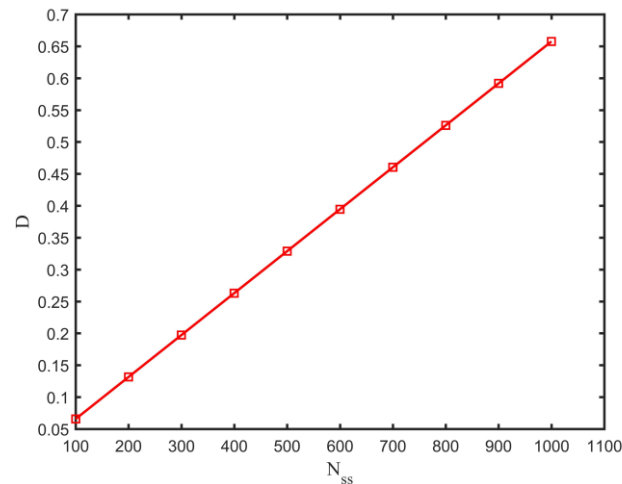


Figure 11. The fatigue damage for various numbers of start-up and shut-down cycles.

If the fatigue damage at failure is 1, the fatigue damage is acceptable even for $N_{ss} = 1000$. However, if the fatigue damage at failure is 0.1, which is usually used in off-shore pipelines and risers, only about 150 start-up and shut-down cycles are allowed during the service life of the pipeline, indicating the necessity of fatigue strength assessment.

5. Conclusions

The following conclusions may be established:

1. For the fully constrained condition, the longitudinal stress range due to start-up and shut-down cycles depends on the variation of internal pressure and temperature. Increasing the operating internal pressure and increasing the operating temperature has the opposite effect on the longitudinal stress range.
2. For the study case, the plastic behaviour of the weld root is only significant for severe local stress concentrations. If the local stress concentration is kept at a low level, the HCF approach for fatigue strength assessment can also be used.
3. For single-sided girth welds, the axial misalignment, weld root angle, and weld root bead width are the main geometrical parameters influencing the notch stress factor of the weld root.
4. If the fatigue damage at failure is 0.1, a limited number of start-up and shut-down cycles are allowed during the service life of the pipeline for the study case, indicating the necessity of fatigue strength assessment.
5. There still exist some unsolved problems for the fatigue strength assessment of single-sided girth welds subjected to start-up and shut-down cycles. Some assumptions are made to simplify the fatigue problem and may be used in engineering practice. Further investigations are still required.

Author Contributions: Software, G.J.; formal analysis, G.J.; investigation, X.L.; data curation, G.J.; writing—original draft preparation, Y.D.; writing—review and editing, Y.D. and L.F.; visualization, X.L.; supervision, X.L. All authors have read and agreed to the published version of the manuscript.

Funding: The present work is supported by the National Natural Science Foundation of China (Grant No. 52101350).

Conflicts of Interest: The authors declare no conflict of interest.

Nomenclature

A_e	External area of the pipe
A_i	Internal bore area of the pipe
A_s	Cross-sectional area of the pipe
C_1, C_2	S-N curve parameters
E	Young's modulus
FEM	Finite element method
F_{res}	Installation residual lay tension
HCF	High cycle fatigue
HPHT	High-pressure and high-temperature
h	Weld root bead height
K'	Cyclic strength coefficient
K_f	Notch stress factor
LCF	Low cycle fatigue
m_1, m_2	S-N curve parameters
N_f	Fatigue life
n'	Cyclic strain hardening exponent
P_e	External pressure of the pipe
P_i	Operational internal pressure
$P_{i,ins}$	Internal pressure of the pipe during installation
r_p	Ratio between $\Delta\varepsilon_{eff}$ and $\Delta\varepsilon_{eff,e}$
T_a	Ambient temperature
T_{op}	Operational temperature
t	Wall thickness
W_e	Weld toe bead width
W_i	Weld root bead width
α	Thermal expansion coefficient
μ	Generalised Poisson's ratio
ν	Poisson's ratio
$\Delta\varepsilon_{eff}$	Effective notch strain range
$\Delta\varepsilon_{eff,e}$	Elastic effective notch strain range
$\Delta\sigma_l$	Longitudinal stress range
$\Delta\sigma_n$	Nominal stress range
δ	Axial misalignment
θ	Weld root angle
ρ_f	Fictitious notch radius
σ_{eff}	Effective notch stress
σ_l	Longitudinal stress
$\sigma_{l,ins}$	Longitudinal stress for the installation condition
$\sigma_{l,op}$	Longitudinal stress for the operational condition

References

- Bai, Q.; Bai, Y. *Subsea Pipeline Design, Analysis, and Installation*; Gulf Professional Publishing: Houston, TX, USA, 2014.
- Hong, Z.; Liu, R.; Liu, W.; Yan, S. A lateral global buckling failure envelope for a high temperature and high pressure (HT/HP) submarine pipeline. *Appl. Ocean Res.* **2015**, *51*, 117–128. [[CrossRef](#)]
- Carr, M.; Sinclair, F.; Bruton, D. Pipeline walking-understanding the field layout challenges, and analytical solutions developed for the SAFEBUCK JIP. In Proceedings of the Offshore Technology Conference, Houston, TX, USA, 1–4 May 2006.
- Hasan, S.; Sweet, L.; Hults, J.; Valbuena, G.; Singh, B. Corrosion risk-based subsea pipeline design. *Int. J. Press. Vessel. Pip.* **2018**, *159*, 1–14. [[CrossRef](#)]
- Bai, Q.; Pan, J. Pipeline Fatigue and Fracture Design. In *Encyclopedia of Maritime and Offshore Engineering*; John Wiley & Sons Ltd.: Hoboken, NJ, USA, 2017; pp. 1–18.

6. Heo, J.; Kang, J.; Kim, Y.; Yoo, I.; Kim, K.; Urm, H. A study on the design guidance for low cycle fatigue in ship structures. In Proceedings of the 9th Symposium of Practical Design of Ships and Other Floating Structures, Luebeck-Travemuende, Germany, 12–17 September 2004.
7. Wang, X.; Kang, J.-K.; Kim, Y.; Wirsching, P.H. Low cycle fatigue analysis of marine structures. In Proceedings of the ASME 2006 25th International Conference on Offshore Mechanics and Arctic Engineering, Hamburg, Germany, 4–9 June 2006; pp. 523–527.
8. Dong, P.; Pei, X.; Xing, S.; Kim, M. A structural strain method for low-cycle fatigue evaluation of welded components. *Int. J. Press. Vessel. Pip.* **2014**, *119*, 39–51. [[CrossRef](#)]
9. Pei, X.; Dong, P.; Xing, S. A structural strain parameter for a unified treatment of fatigue behaviors of welded components. *Int. J. Fatigue* **2019**, *124*, 444–460. [[CrossRef](#)]
10. Lawrence, F.; Ho, N.; Mazumdar, P.K. Predicting the fatigue resistance of welds. *Annu. Rev. Mater. Sci.* **1981**, *11*, 401–425. [[CrossRef](#)]
11. Dong, Y.; Garbatov, Y.; Guedes Soares, C. Strain-based fatigue reliability assessment of welded joints in ship structures. *Mar. Struct.* **2021**, *75*, 102878. [[CrossRef](#)]
12. Saiprasertkit, K.; Hanji, T.; Miki, C. Fatigue strength assessment of load-carrying cruciform joints with material mismatching in low-and high-cycle fatigue regions based on the effective notch concept. *Int. J. Fatigue* **2012**, *40*, 120–128. [[CrossRef](#)]
13. Dong, Y.; Garbatov, Y.; Guedes Soares, C. Improved effective notch strain approach for fatigue reliability assessment of load-carrying fillet welded cruciform joints in low and high cycle fatigue. *Mar. Struct.* **2021**, *75*, 102849. [[CrossRef](#)]
14. Ngoula, D.T.; Beier, H.T.; Vormwald, M. Fatigue crack growth in cruciform welded joints: Influence of residual stresses and of the weld toe geometry. *Int. J. Fatigue* **2017**, *101*, 253–262. [[CrossRef](#)]
15. Hutař, P.; Poduška, J.; Šmíd, M.; Kuběna, I.; Chlupová, A.; Náhlík, L.; Polák, J.; Kruml, T. Short fatigue crack behaviour under low cycle fatigue regime. *Int. J. Fatigue* **2017**, *103*, 207–215. [[CrossRef](#)]
16. Cheng, A.; Chen, N.-Z.; Pu, Y.; Yu, J. Fatigue crack growth prediction for small-scale yielding (SSY) and non-SSY conditions. *Int. J. Fatigue* **2020**, *139*, 105768. [[CrossRef](#)]
17. Cheng, A.; Chen, N.-Z. Structural integrity assessment for deep-water subsea pipelines. *Int. J. Press. Vessel. Pip.* **2022**, *199*, 104711. [[CrossRef](#)]
18. Schweizer, C.; Seifert, T.; Nieweg, B.; Von Hartrott, P.; Riedel, H. Mechanisms and modelling of fatigue crack growth under combined low and high cycle fatigue loading. *Int. J. Fatigue* **2011**, *33*, 194–202. [[CrossRef](#)]
19. Deng, J.; Yang, P.; Dong, Q.; Wang, D. Research on CTOD for low-cycle fatigue analysis of central-through cracked plates considering accumulative plastic strain. *Eng. Fract. Mech.* **2016**, *154*, 128–139. [[CrossRef](#)]
20. Fricke, W. *IIW Recommendations for the Fatigue Assessment of Welded Structures by Notch Stress Analysis: IIW-2006-09*; Woodhead Publishing: Shaston, UK, 2012.
21. Glinka, G. Calculation of inelastic notch-tip strain-stress histories under cyclic loading. *Eng Fract Mech* **1985**, *22*, 839–854. [[CrossRef](#)]
22. Glinka, G. Energy density approach to calculation of inelastic strain-stress near notches and cracks. *Eng. Fract. Mech.* **1985**, *22*, 485–508. [[CrossRef](#)]
23. Dowling, N.E. *Mechanical Behavior of Materials: Engineering Methods for Deformation, Fracture, and Fatigue*; Pearson: London, UK, 2013.
24. Fatoba, O.; Akid, R. Low cycle fatigue behaviour of API 5L X65 pipeline steel at room temperature. *Procedia Eng.* **2014**, *74*, 279–286. [[CrossRef](#)]
25. Dong, Y.; Garbatov, Y.; Guedes Soares, C. Fatigue strength assessment of an annealed butt welded joint accounting for material inhomogeneity. In *Progress in the Analysis and Design of Marine Structures*; Guedes Soares, C., Garbatov, Y., Eds.; Taylor & Francis Group: London, UK, 2017; pp. 349–359.
26. Horn, A.M.; Lotsberg, I.; Orjaseater, O. The rationale for update of SN curves for single sided girth welds for risers and pipelines in DNV GL RP C-203 based on fatigue performance of more than 1700 full scale fatigue test results. In Proceedings of the International Conference on Ocean, Offshore and Arctic Engineering (OMAE), Madrid, Spain, 17–22 June 2018.
27. Zhang, Y.-H.; London, T.; DeBono, D. Developing Mk Solutions for Fatigue Crack Growth Assessment of Flaws at Weld Root Toes in Girth Welds. In Proceedings of the International Conference on Offshore Mechanics and Arctic Engineering, Madrid, Spain, 17–22 June 2018.
28. Dong, Y.; Kong, X.; An, G.; Kang, J. Fatigue reliability of single-sided girth welds in offshore pipelines and risers accounting for non-destructive inspection. *Mar. Struct.* **2022**, *86*, 103268. [[CrossRef](#)]
29. ANSYS. Online Manuals. 2012.
30. Dong, Y.; Teixeira, A.P.; Guedes Soares, C. Fatigue reliability analysis of butt welded joints with misalignments based on hotspot stress approach. *Mar. Struct.* **2019**, *65*, 215–228. [[CrossRef](#)]
31. Hobbacher, A. *Recommendations for Fatigue Design of Welded Joints and Components*; Springer: Berlin/Heidelberg, Germany, 2015.
32. DNVGL. *Fatigue Design of Offshore Steel Structures*; Det Norske Veritas: Hovik, Norway, 2016; Volume DNVGL-RP-C203.